ChemComm

The efficiency of 18F labelling of prostate specific membrane antigen ligand via strain-promoted azide-alkyne reaction: reaction speed versus hydrophilicity

Journal:	*ChemComm*
Manuscript ID	CC-COM-05-2018-003999.R1
Article Type:	Communication

ChemComm

COMMUNICATION

The efficiency of ^{18}F labelling of prostate specific membrane antigen ligand via strain-promoted azide-alkyne reaction: reaction speed versus hydrophilicity.

Received 00th January 20xx,
Accepted 00th January 20xx

DOI: 10.1039/x0xx00000x

www.rsc.org/

Mengzhe Wang,[a] Christopher D. McNitt,[b] Hui Wang,[a] Xiaofen Ma,[a,c]* Sarah M. Scarry,[d] Zhanhong Wu,[a] Vladimir V. Popik,[b,] * and Zibo Li[a,] *

Here we report the ^{18}F labeling of prostate specific membrane antigen ligand (PSMA) via strain promoted oxa-dibenzocyclooctyne (ODIBO)- or bicyclo[6.1.0]nonyne (BCN)-azide reaction. Although ODIBO reacts with azide 20 fold faster than BCN, *in vivo* PET imaging suggests ^{18}F-BCN-Azide-PSMA demonstrated much higher tumor uptake and tumor to background contrast.

Positron emission tomography (PET) is a powerful imaging technology that enables the visualization and quantification of target expression, metabolic perturbations, and many other biological processes in vivo.[1] Of the commonly used PET radionuclides, ^{18}F is the most broadly utilized due to its ideal chemical, physical and nuclear properties.[2] Despite the great promise, the short half-life of ^{18}F (~110 min) and the poor nucleophilicity of fluoride make it difficult to directly incorporate ^{18}F into complex molecules. Significant amount of effort was therefore devoted to the development of highly efficient ^{18}F labelling methods for PET probe construction.[3]

In the past decades, bioorthogonal reactions have become a unique tool in diverse fields including nuclear medicine.[4, 5] In particular, copper(I) (Cu(I)) catalysed azide-alkyne reactions was found to be rapid and clean which has also been successfully adapted to ^{18}F radiolabelling of various biologically active agents.[6] However, the use of cytotoxic copper catalyst in reaction complicated quality control process since Cu(I) could lead to oligonucleotide and polysaccharide degradation in vivo.[7-9] To address this limitation, azide based metal-free click reactions have been developed including covalent ligation of azide to phosphines and strain-promoted cycloaddition of azide to alkynes (such as cyclooctynes, dibenzocyclooctynes, azadibenzocylcooctynes and thia-cycloalkynes).[10-14] Unfortunately, phosphines suffered from oxygen sensitivity, while some commonly used cyclooctynes showed slow kinetics, and required lengthy synthetic routes for preparation.[12, 15-17] Previously the Popik group reported the synthesis of oxa-dibenzocyclooctynes (ODIBO), which is one of the most reactive cyclooctynes (>45 M^{-1} s^{-1}) for strain promoted azide cycloaddition.[18] This ultrafast reaction was also converted to an attractive ^{18}F labelling method that allows extremely fast conjugation of ^{18}F-ODIBO to azide-tagged peptides and proteins.[19] In this study, we perform side by side comparison between ^{18}F-ODIBO and ^{18}F-bicyclo[6.1.0]nonyne (^{18}F-BCN) [20, 21] on PET probe construction. Both reaction rate and probe hydrophilicity are explored for ^{18}F labelling of PSMA ligands. The obtained information may provide guidance on selecting appropriate labelling method for PET probe construction.

As shown in Scheme 1, ^{18}F-ODIBO (^{18}F-**2**) was obtained in

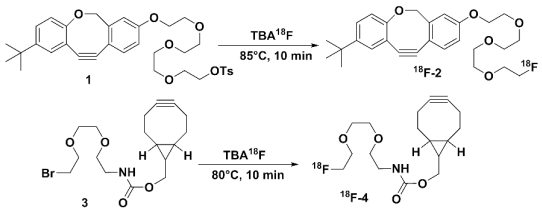

Scheme 1. Labeling scheme for ^{18}F-ODIBO (^{18}F-**2**) and ^{18}F-BCN (^{18}F-**4**)

5.6 ± 1.1% non-decay corrected isolation yield with >99% radiochemical purity according to a previously reported protocol (Figure 1a).[18] The co-injection with ^{19}F-**2** standard confirmed its identity (Figure S1). Although ^{18}F-labeled BCN has been reported before,[20, 21] we use a modified method to achieve ^{18}F-**4** bearing an extra ethylene glycol unit to enhance BCN's aqueous solubility. In brief, starting from the bromo-precursor, nucleophilic substitution was performed using different solvents, temperature and time. As shown in Table 1, DMSO and THF result in lower labelling yield compared with

[a] Department of Radiology and Biomedical Research Imaging Center, University of North Carolina at Chapel Hill, Chapel Hill, North Carolina 27599, USA Email: zibo_li@med.unc.edu
[b] Department of Chemistry, University of Georgia, Athens Georgia 30602, USA. Email: vpopik@uga.edu
[c] Department of Medical Imaging, Guangdong Second Provincial General Hospital, Guangzhou, Guangdong, China, 510317, Email: xiaofenma12@163.com
[d] Division of Chemical Biology and Medicinal Chemistry, UNC Eshelman School of Pharmacy, University of North Carolina at Chapel Hill, Chapel Hill, North Carolina 27599, USA

Electronic Supplementary Information (ESI) available: [details of any supplementary information available should be included here]. See

MeCN. The optimal reaction temperature is 80°C within the tested conditions. Significant amount of unreacted bromo precursor was observed at room temperature and 60°C, indicating insufficient labelling reaction rate. Further increase the temperature to 100°C lead to decreased labelling yield which could be caused by the increased side reaction of Br-elimination and decomposition of BCN motif. We would like to point out that the yield determined here are isolation yield, which is more relevant to real practice, but much lower than yield determined by radio TLC: the non-specific bindings of product to HPLC lines and HPLC columns during purification will lower the yield. A 99% radiochemical purity could be obtained after purification (Figure 1b).

Table 1 Labelling conditions for ^{18}F-**4**

	Solvent	T(°C)	Time/min	Isolation Yield%
1	DMSO	80	10	5
2	THF	80	10	1
3	MeCN	r.t.	10	0
4	MeCN	60	10	0
5	MeCN	80	10	8
6	MeCN	100	10	4
7	MeCN	80	20	8
8	MeCN	80	30	9

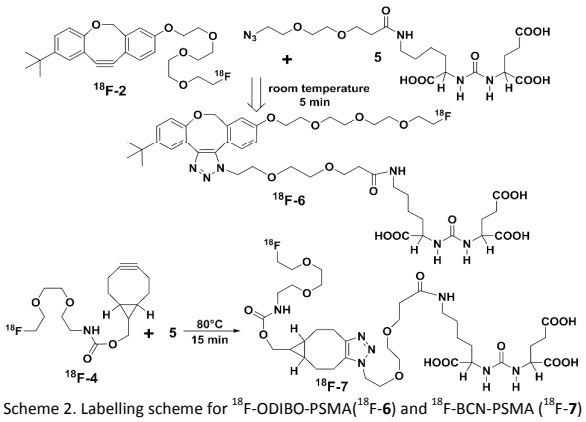

Scheme 2. Labelling scheme for ^{18}F-ODIBO-PSMA(^{18}F-**6**) and ^{18}F-BCN-PSMA (^{18}F-**7**)

Recognizing the short half-life of ^{18}F, recent effort on new labelling method development has been mainly focused on improving reaction rate. With ^{18}F-**2** and ^{18}F-**4** on hand, we explore the factors that should be considered when selecting appropriate methods for PET probe construction. The major difference between ^{18}F-**2** and ^{18}F-**4** are ODIBO reacts with azide 20-fold faster than BCN; and ^{18}F-**4** is more hydrophilic than ^{18}F-**2** (Figure 1). The target of interest in our approach is prostate specific membrane antigen (PSMA), which was found to be over expressed in prostate cancer with limited expression in healthy tissues.[22-29] As shown in Scheme 2, ^{18}F-**2** and ^{18}F-**4** could react with azide-PSMA ligand to achieve ^{18}F-PSMA ligands.

Due to the fast kinetic of the reaction between the ^{18}F-**2** and azide(**5**), we were able to obtain ^{18}F-**6** in 20 ± 1% isolated yield with only 10 μg of **5** at neutral condition, room temperature and within seconds. In contrast, the ^{18}F-**4** reacts much slower with **5**. Five-fold larger amount of **5**, longer reaction time (15 min) and higher temperature (80°C) are needed to obtain reasonable yield (Table 2). Both reactions could proceed at pH 5.5, 7.0 and pH 8.5. In order to determine the effect of prosthetic group on the lipophilicity of the final PET agents, octanol-water partition coefficient of ^{18}F-**6** and ^{18}F-**7** was first evaluated. The log P values of ^{18}F-**6** and ^{18}F-**7** ^{18}are -2.03 ± 0.01 and -2.62 ± 0.04, respectively. This correlates well with our expectation that the more hydrophobic ODIBO will lead to more lipophilic product. In addition to the difference in hydrophilicity, the size of the hydrophobic motif and the length of hydrophilic polyethylene glycol chain may also lead to difference in the amphiphilic properties of the two compounds and further affect their biodistribution in vivo.

Table 2 Labelling conditions for ^{18}F-**7**

	T(°C)	Amount of PSMA-N_3/μg	pH	Isolation Yield%
1	r.t.	50	7.0	5
2	40	50	7.0	26
3	60	50	7.0	32
4	80	50	7.0	36
5	40	10	7.0	Not Detected
6	40	50	5.5	21
7	40	50	8.5	26

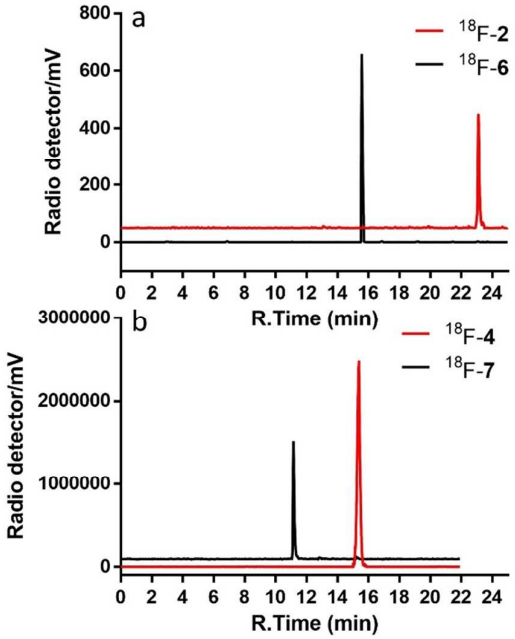

Figure 1 Radio HPLC profile of (a) ^{18}F-**2** and ^{18}F-**6**. (b) ^{18}F-**4** and ^{18}F-**7**

In order to confirm that target binding affinity was still maintained after the peptide modification, we compared the in vitro cell binding affinity of ^{19}F-**6** and ^{19}F-**7** with that of the clinically used PSMA-617 via competitive cell binding assay. As shown in Figure 2, all the compounds inhibited the binding in a dose-dependent manner. As the reference, PSMA-617 had the 50% inhibitory concentration (IC_{50}) as 144.6 nM while the IC_{50} values of ^{19}F-**6** and ^{19}F-**7** are 108.9 nM and 156.4 nM, respectively. The comparable IC_{50} values demonstrated that

both ^{19}F-**6** and ^{19}F-**7** have similar binding affinity compared with PSMA-617 and could be further evaluated *in vivo*.

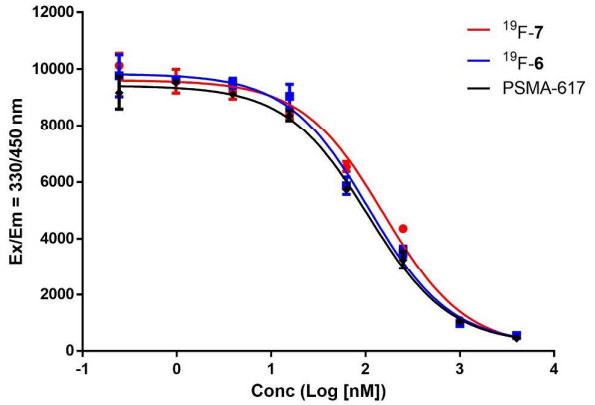

Figure 2 Competitive binding assay of ^{19}F-**6** and ^{19}F-**7** compared with PSMA-617 as reference

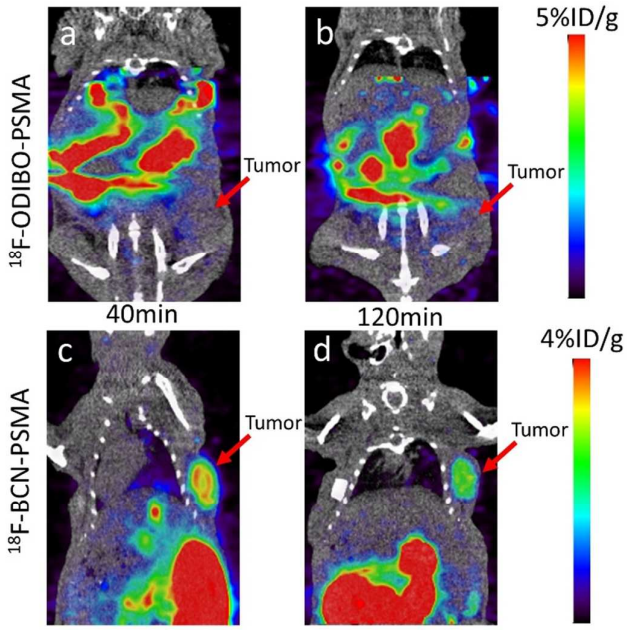

Figure 3 Representative PET/CT images of (a)(b) LNCap xenograft at 40min and 120min post injection of ^{18}F-**6**, respectively and (c)(d) LNCap xenograft at 40min and 120min post injection of ^{18}F-**7**, respectively

The targeting efficiency of ^{18}F-**6** and ^{18}F-**7** was evaluated by performing multiple time-point static microPET scans in PSMA positive LNCap tumor-bearing mice (n=3). After administration of 3.7 MBq of either ^{18}F-**6** or ^{18}F-**7** via tail vein, animals were scanned at 40 min and 120 min post injection. As shown in Figure 3a and 3b, although ^{18}F-**6** demonstrated good PSMA affinity in binding assay, very low uptake can be seen in the tumor region in vivo. The tumor uptake was only 0.46 ± 0.02 % ID/g and 0.30 ± 0.01 % ID/g at 40 min and 120 min post injection, respectively. Radio signals were mainly localized at gallbladder and intestines, which could be caused by the relatively more hydrophobic ODIBO motif of ^{18}F-**6** or the stability of the reagent. On the contrary, tumor can be clearly visualized by ^{18}F-**7** PET (Figure 3c and 3d). The tumor uptake was 2.49 ± 0.34 % ID/g and 2.24 ± 0.03 % ID/g at 40 min and 120 min post injection, which was significantly higher than those of ^{18}F-**6** at both time points (p=0.01 for 40 min and p=0.0001 for 120 min time points). Although uptake was still visible in gallbladder and intestine, kidney is the organ with higher tracer uptake. This observation could be attributed to the more hydrophilic BCN motif of ^{18}F-**7** and the background PSMA expression in kidneys.[30, 31] Quantitative analysis of major organs are shown in Figure 4. At 120 min p.i., the tumor to liver, tumor to muscle ratios are 0.24 ± 0.01 and 2.47 ± 0.90 for ^{18}F-**6** respectively. On the other hand, the contrast are 5.83 ± 1.5 and 69.59 ± 7.23 for ^{18}F-**7** respectively. This led to clean PET images and high tumor to background ratio.

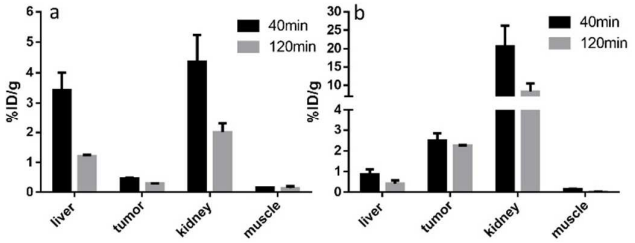

Figure 4 Quantitative uptake of major organs in LNCap xenografts post injection of (a) ^{18}F-**6** and (b) ^{18}F-**7**

The targeting specificity of ^{18}F-**7** was confirmed by a blocking study in which excess amount of unradiolabeld PSMA ligand was coinjected with the tracer. As shown in Figure 5, the tumor uptake in blocking group was significantly reduced compared with that of in the normal group (p=0.04). This demonstrated that the unradiolabeled PSMA ligand successfully blocked the targeting sites and reduced the tracer uptake in the blocking group.

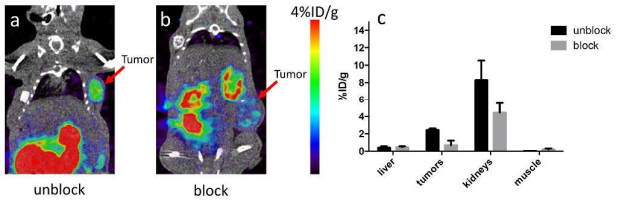

Figure 5 Representative PET/CT images of LNCap xenograft at 120min post injection of ^{18}F-**7** (a) without and (b)with a blocking dose. Quantitative uptake of major organs derived from PET images.

Conclusion: Due to the short half-life of ^{18}F, significant amount of effort has recently been devoted to the development of ultrafast labelling reactions. In this study, we used a highly reactive but more hydrophobic ^{18}F-**2** and a less reactive but more hydrophilic ^{18}F-**4** to construct PSMA targeting PET probes via azide-alkyne click reaction. Both agents could be efficiently prepared and demonstrated comparable target binding affinity in vitro. However, ^{18}F-**6** failed to provide reasonable tumor to background contrast potentially due to the hydrophobicity of ODIBO motif. The more hydrophilic BCN derived tracer showed much higher tumor uptake and tumor to background ratio. The information obtained here suggest both reaction speed and hydrophilicity should be considered when selecting appropriate labeling methods for PET probe construction. ^{18}F-**2** might be more suitable for protein labeling which require fast reaction rate

but may be less affected by hydrophobicity of labeling motif due to the large molecular weight. Nonetheless, other factors including position of modification, degree of modification, and charge change could all affect the distribution of the final agents.

Conflicts of interest

There are no conflicts to declare.

Notes and references

‡ This work was supported by UNC Chapel Hill Department of Radiology and BRIC, NSF grant (CHE-1565646), and the Science and Technology Program of Guangzhou, china (grant number: 201804010448). Financial support for the PSMA ligand synthesis in the form of start-up funding awarded from the UNC-CH to Professor Jeffrey Aubé is gratefully acknowledged. We thank the UNC-CH Department of Chemistry Mass Spectrometry Core Lab, especially Brandie M. Ehrmann and Karl M. Koshlap in the UNC ESOP NMR Core Facility (PSMA ligand data).

1. S. M. Ametamey, M. Honer and P. A. Schubiger, *Chem Rev*, 2008, **108**, 1501-1516.
2. Z. Li and P. S. Conti, *Adv Drug Deliv Rev*, 2010, **62**, 1031-1051.
3. H. S. Krishnan, L. Ma, N. Vasdev and S. H. Liang, *Chemistry*, 2017, **23**, 15553-15577.
4. K. Lang and J. W. Chin, *ACS Chem Biol*, 2014, **9**, 16-20.
5. J. P. Meyer, P. Adumeau, J. S. Lewis and B. M. Zeglis, *Bioconjug Chem*, 2016, **27**, 2791-2807.
6. M. Meldal and C. W. Tornøe, *Chemical Reviews*, 2008, **108**, 2952-3015.
7. J. Gierlich, G. A. Burley, P. M. E. Gramlich, D. M. Hammond and T. Carell, *Organic Letters*, 2006, **8**, 3639-3642.
8. E. Lallana, E. Fernandez-Megia and R. Riguera, *Journal of the American Chemical Society*, 2009, **131**, 5748-5750.
9. A. J. Link, M. K. S. Vink and D. A. Tirrell, *Journal of the American Chemical Society*, 2004, **126**, 10598-10602.
10. G. de Almeida, E. M. Sletten, H. Nakamura, K. K. Palaniappan and C. R. Bertozzi, *Angewandte Chemie International Edition*, 2012, **51**, 2443-2447.
11. J. Dommerholt, S. Schmidt, R. Temming, L. J. A. Hendriks, F. P. J. T. Rutjes, J. C. M. van Hest, D. J. Lefeber, P. Friedl and F. L. van Delft, *Angewandte Chemie International Edition*, 2010, **49**, 9422-9425.
12. M. Köhn and R. Breinbauer, *Angewandte Chemie*, 2004, **116**, 3168-3178.
13. A. Kuzmin, A. Poloukhtine, M. A. Wolfert and V. V. Popik, *Bioconjugate Chemistry*, 2010, **21**, 2076-2085.
14. X. Ning, J. Guo, M. A. Wolfert and G.-J. Boons, *Angewandte Chemie (International ed. in English)*, 2008, **47**, 2253-2255.
15. J. A. Codelli, J. M. Baskin, N. J. Agard and C. R. Bertozzi, *Journal of the American Chemical Society*, 2008, **130**, 11486-11493.
16. M. F. Debets, S. S. van Berkel, S. Schoffelen, F. P. J. T. Rutjes, J. C. M. van Hest and F. L. van Delft, *Chemical Communications*, 2010, **46**, 97-99.
17. J. C. Jewett, E. M. Sletten and C. R. Bertozzi, *Journal of the American Chemical Society*, 2010, **132**, 3688-3690.
18. C. D. McNitt and V. V. Popik, *Org Biomol Chem*, 2012, **10**, 8200-8202.
19. M. Boudjemeline, C. D. McNitt, T. A. Singleton, V. V. Popik and A. P. Kostikov, *Organic & Biomolecular Chemistry*, 2018, DOI: 10.1039/C7OB02532G.
20. X.-G. Li, C. Hagert, R. Siitonen, H. Virtanen, O. Sareila, H. Liljenbäck, J. Tuisku, J. Knuuti, J. Bergman, R. Holmdahl and A. Roivainen, *ACS Medicinal Chemistry Letters*, 2016, **7**, 826-830.
21. X. G. Li, A. Roivainen, J. Bergman, A. Heinonen, F. Bengel, T. Thum and J. Knuuti, *Chem Commun (Camb)*, 2015, **51**, 9821-9824.
22. H. J. K. Ananias, M. C. van den Heuvel, W. Helfrich and I. J. de Jong, *The Prostate*, 2009, **69**, 1101-1108.
23. S. Minner, C. Wittmer, M. Graefen, G. Salomon, T. Steuber, A. Haese, H. Huland, C. Bokemeyer, E. Yekebas, J. Dierlamm, S. Balabanov, E. Kilic, W. Wilczak, R. Simon, G. Sauter and T. Schlomm, *The Prostate*, 2011, **71**, 281-288.
24. M. Rybalov, H. J. K. Ananias, H. D. Hoving, H. G. van der Poel, S. Rosati and I. J. de Jong, *International Journal of Molecular Sciences*, 2014, **15**, 6046-6061.
25. A. Afshar-Oromieh, H. Hetzheim, C. Kratochwil, M. Benesova, M. Eder, O. C. Neels, M. Eisenhut, W. Kübler, T. Holland-Letz, F. L. Giesel, W. Mier, K. Kopka and U. Haberkorn, *Journal of Nuclear Medicine*, 2015, **56**, 1697-1705.
26. A. Afshar-Oromieh, T. Holland-Letz, F. L. Giesel, C. Kratochwil, W. Mier, S. Haufe, N. Debus, M. Eder, M. Eisenhut, M. Schäfer, O. Neels, M. Hohenfellner, K. Kopka, H.-U. Kauczor, J. Debus and U. Haberkorn, *European Journal of Nuclear Medicine and Molecular Imaging*, 2017, **44**, 1258-1268.
27. C. Cui, M. Hanyu, A. Hatori, Y. Zhang, L. Xie, T. Ohya, M. Fukada, H. Suzuki, K. Nagatsu, C. Jiang, R. Luo, G. Shao, M. Zhang and F. Wang, *American Journal of Nuclear Medicine and Molecular Imaging*, 2017, **7**, 40-52.
28. B. Grubmüller, R. P. Baum, E. Capasso, A. Singh, Y. Ahmadi, P. Knoll, A. Floth, S. Righi, S. Zandieh, C. Meleddu, S. F. Shariat, H. C. Klingler and S. Mirzaei, *Cancer Biotherapy and Radiopharmaceuticals*, 2016, **31**, 277-286.
29. C. Uprimny, *Wien Med Wochenschr*, 2017, DOI: 10.1007/s10354-017-0569-z.
30. Y. Kinoshita, K. Kuratsukuri, S. Landas, K. Imaida, P. M. Rovito, Jr., C. Y. Wang and G. P. Haas, *World J Surg*, 2006, **30**, 628-636.
31. S. O'Keefe Denise, J. Bacich Dean and D. W. Heston Warren, *The Prostate*, 2003, **58**, 200-210.